ChemComm

Accepted Manuscript

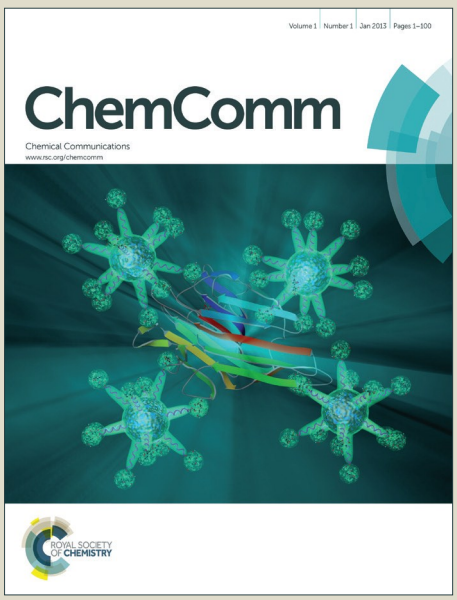

ROYAL SOCIETY OF CHEMISTRY

www.rsc.org/chemcomm

Journal Name

ARTICLE

A Phosphinate-Based Near-Infrared Fluorescence Probe for Imaging the Superoxide Radical Anion in *In Vitro* and *In Vivo*

Received 00th January 20xx,
Accepted 00th January 20xx

DOI: 10.1039/x0xx00000x

www.rsc.org/

Jianjian Zhang,[a] Chuwen Li,[b] Rui Zhang,[a] Fengyuan Zhang,[a] Wei Liu,[a] Xiaoyan Liu,[a] Simon Ming-Yuen Lee,[b] and Haixia Zhang*[a]

A novel near-infrared (NIR), turn-on fluorescence probe **CyR** containing a phosphinate group as recognizing moiety for selective detection $O_2^{\bullet-}$ with a low limit of detection (LOD, 9.9 nM) was developed. **CyR** has good cell-membrane permeability, intracellular stability, and low cytotoxicity. In addition, we have successfully applied the CyR to visualize $O_2^{\bullet-}$ in live zebrafish, mouse and, for the first time, in mouse liver.

Introduction

Reactive oxygen species (ROSs), the natural by-products of oxidative energy metabolism, are often considered as the active oxygen free radicals and other substances which can be transformed into free radical. They are of crucial importance for a wide variety of cellular functions.[1] ROSs are involved in the immune process and have a key role in organism defense against exogenous microbes such as bacteria, viruses, parasites, and so on.[2] They are a broad range of small signaling molecules containing highly reactive unpaired valence or odd number of electrons. ROSs include superoxide ($O_2^{\bullet-}$), hydrogen peroxide (H_2O_2), hydroxyl radical (•OH), and peroxynitrite ($ONOO^-$).[3] Although ROSs have some biological preponderances, excessive generation may threaten threatened homeostasis of the biosystem,[4] and lead to the development of age-dependent diseases such as neurodegenerative disorders, cancer, arthritis, arteriosclerosis, oxidative stress and others.[5] The superoxide radical ($O_2^{\bullet-}$) is the precursor of most of the reactive oxygen or nitrogen species (ROS or RNS) found in cells.[6] Superoxide radical ($O_2^{\bullet-}$) can get hydrogen peroxide (H_2O_2) by disproportionation,[7] and generate $ONOO^-$ through oxidization in the existence of NO.[8] Hence, it is significant to illuminate the relationship between $O_2^{\bullet-}$ fluxes and diseases. However, the identification and quantification of $O_2^{\bullet-}$ with high selectivity and sensitivity remains an obstacle.

The generally described efforts devoted to determining $O_2^{\bullet-}$ include mass spectrometry (MS), high performance liquid chromatography (HPLC), electron paramagnetic resonance spectroscopy (EPR), etc.[9] However, all the analytical methods are time-consuming and complex and/or require special equipment. Besides, they are only suitable for extracellular detection. Various fluorescence and chemiluminescent probes[10] have been widely used due to their simplicity and high sensitivity. They also have capability to image in *in vitro* and even *in vivo* owing to their non-invasion.[11] Most reaction-based fluorescence sensors were developed based on the oxidation capability[10a-f] and strong nucleophilicity[10g-k] of $O_2^{\bullet-}$ (Table S1). Several challenging problems in the development of fluorescent probes for $O_2^{\bullet-}$ are still unsolved: (i) selectivity over competing ROS such as H_2O_2, $ONOO^-$, and •OH, (ii) fast response within a few minutes, (iii) high sensitivity to detect the endogenously produced $O_2^{\bullet-}$, (iv) biocompatibility such as cell permeability, intracellular stability, and low toxicity, and (v) signaling in the biological tissue optical window. Unfortunately, the existing probes hardly meet all of these requirements. Hence, designing practical fluorescence probe for $O_2^{\bullet-}$ and visualizing $O_2^{\bullet-}$ in living cells and in vivo is in urgent need.

A few of fluorescence probes based on the oxidation properties of $O_2^{\bullet-}$ have been designed.[10a-f] In 1984, Gallop *et al.*[12] reported that hydroethidine (HE) was readily taken up and accumulated by live cells. Then HE grafted into nucleic acid, where HE could be oxidized to ethidium (Etd^+; 3,8-diamino-5-ethyl-6-phenylphenanthridinium), greatly strengthening its fluorescence.[13] However, in 1990, Rothe and Valet[14] showed *in vitro* that HE was oxidized by potassium superoxide (KO_2). They also demonstrated that HE was oxidized not only by $O_2^{\bullet-}$ but also by H_2O_2 plus peroxidase. Hence, the major drawback of HE was its limit for the quantitative measurement of $O_2^{\bullet-}$. Taking advantage of the $O_2^{\bullet-}$-induced deprotection of diphenyl phosphinated and sulfonylated fluoresceins, a series of excellent fluorescent chemodosimeters for $O_2^{\bullet-}$ have been developed.[10g-k] Tang's group[10j, k] designed two phosphinate-based dyes, which exhibit high selectivity for $O_2^{\bullet-}$ over other ROSs and some biological compounds. The dyes have been successfully used for imaging $O_2^{\bullet-}$ in live mouse peritoneal macrophages. Furthermore, Maeda *et al.*[10i] developed a $O_2^{\bullet-}$ probe using deprotection of 2,4-Dinitrobenzenesulfonyl group. It can be detected in neutrophils by fluorescence microscopy. But it also responded to thiols and reductases, which restricted its use in the specific measurement of $O_2^{\bullet-}$ in real biological systems. Most of the currently probes for highly selectivity of $O_2^{\bullet-}$ have been developed, however, they had higher detection limit[10a,c,h], high ratio of organic

[a] *State Key Laboratory of Applied Organic Chemistry, Key Laboratory of Nonferrous Metals Chemistry and Resources Utilization of Gansu Province and College of Chemistry and Chemical Engineering, Lanzhou University, Lanzhou 730000, China, Tel.: +86 931 8912510; fax: +86 931 8912582,*
E-mail address: zhanghx@lzu.edu.cn.
[b] *State Key Laboratory of Quality Research in Chinese Medicine and Institute of Chinese Medical Sciences, University of Macau, Macao, China.*
†Electronic Supplementary Information (ESI) available: Detailed procedures, characterization data, and additional plots. See DOI: 10.1039/x0xx00000x

solvents[10c,h,i], narrow linear region[10d,k], or excitation wavelength located in ultraviolet–visible[10a,c,d,g-j]. Therefore, the detection of superoxide with high sensitivity and selectivity is an ongoing challenge.

In this report, we present a novel flurescent probe for superoxide detection based on phosphinate. The probe displays a large wavelength shift on UV spectra and visible color change with naked-eye for highly selective detection of $O_2^{\bullet-}$ over competing ROSs. The probe also has capability to image micromolar changes in $O_2^{\bullet-}$ concentrations in not only aqueous samples but also biosystem.

Results and Discussion

Synthesis of CyR. **CyR** could be easily synthesized via a two-steps reaction from compound **1** in excellent purity and good yield (66%) shown in Scheme 1. The final product was purified by neutral aluminium oxide column chromatography using CH_2Cl_2/0-20% methanol as eluent and fully characterized by ^{1}H NMR, ^{13}C NMR, ^{31}P NMR, IR, and HRMS (Supporting Information).

After the reaction of SOD (Superoxide Dismutase, 200 U) with X/XO (xanthine/Xanthine oxidase, final 30 μM/30 mU) in PBS was carried out for 30 min, **CyR** (5 μM) was added into the reactive solution. The mixture was shaken well and kept at 25 °C for 5 min before measurement. As can be seen from Figure 1A(d), the fluorescence intensity was obviously inhibited by SOD addition.

To be helpful in biological applications, it is necessary for a probe to be operational over a suitable range of pH, especially at physiological pH. As shown in Figure S1, it was found that the fluorescence intensities remained nearly the same for **CyR** at pH ranging from 3.0 to 8.0, and changed slightly under alkaline solution. Figure S1 also showed that the optimum pH range was from 7.0 to 8.0. So **CyR** does well in the physiological pH region and pH 7.4 was chosen as the experimental condition.

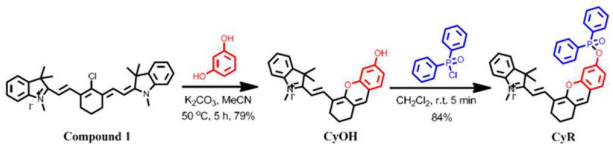

Scheme 1. Synthesis of **CyR**

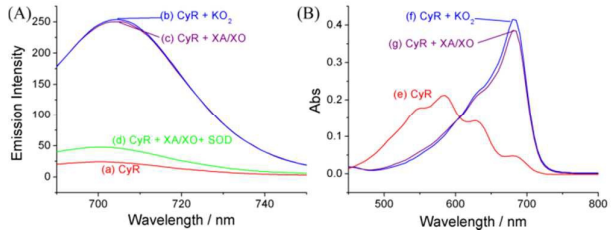

Figure 1. (A) Effect of SOD on fluorescence intensity of the system of **CyR** with superoxide: (a) control, **CyR** (5 μM); (b) KO_2 (final 10 μM) and (c) X/XO (final 30 μM/30 mU) was added into the solution of **CyR** (5 μM) in PBS (10 mM, pH 7.4); (d) after the reaction of SOD (200 U) with X/XO (final 30 μM/30 mU) in PBS was carried out for 30 min, **CyR** (5 μM) was added into the reactive solution; (B) Absorption spectrum of 5 μM **CyR** (e), 5 μM **CyR** with 10 μM KO_2 (f), and with 30 μM/30 mU X/XO (g) in PBS (10 mM, pH 7.4) containing 5% DMSO. (In theory, 1 μM xanthine transforms to 1/3 μM superoxide under physiological conditions.[15])

Specificity of the Probe. To prove the selectivity of **CyR**, the response towards various ROSs, amino acids, metal ions, and reductants was investigated in detail. The fluorescent response of a solution of **CyR** (5 μM) and KO_2 (20 μM) after 2, 5, 10, and 20 min incubation at 25 °C was compared to those of reactions with others ROSs (20 μM ^{t}BuOOH or H_2O_2, 50 μM $ONOO^-$, NO•, •OH, OCl^- or $^1O_2$), amino acids (50 μM Gly, Try, Phe, Thr, Leu, Val, and His), reductants (50 μM 1,4-hydroquinone (HQ), glutathione or Vitamine C) and metal ions (50 μM Fe^{2+}, K^+, Na^+, Ca^{2+}, Mg^{2+}, Cu^{2+}, Zn^{2+}, Al^{3+}). As shown in Figure S2, **CyR** provided a highly specific fluorescent response toward $O_2^{\bullet-}$, while gave a slight response to H_2O_2. This indicated that the reaction of **CyR** with $O_2^{\bullet-}$ was based on nucleophilic substitution and deprotection of phosphinate moiety, not on an oxidative mechanism.

As can be seen from Figure S3, upon addition of different concentration of X/XO (0/0, 0.3/0.3, 1.0/1.0, 3.0/3.0, 8.0/8.0, 15.0/15.0, 20.0/20.0, 30.0/30.0, 45.0/45.0 μM/mU), the aqueous solution of the mixture exhibits very remarkable color change from purple to cyan, admitting the colorimetric detection of $O_2^{\bullet-}$ by the "naked eye". In addition, the response rate of **CyR** to $O_2^{\bullet-}$ was tested by time-course fluorescence measurements (Figure S4A). The fluorescence intensity at 704 nm increased gradually and reached a plateau in approximately 10 min in the presence of $O_2^{\bullet-}$ (20 μM). Besides, **CyR** displayed good photostability for more than 3 h (Figure S4B). Finally, an approximate 10-fold increase in fluorescence intensity was obtained. Based on these results, we affirmed that **CyR** can detect $O_2^{\bullet-}$ rapidly.

Spectra of CyR titrated with $O_2^{\bullet-}$. The response ability of **CyR** to $O_2^{\bullet-}$ was tested. As expected, a steady increase at 704 nm was observed (Figure 2A) when different concentrations of KO_2 (0, 0.25, 0.5, 1.0, 1.5, 2.0, 2.5, 3.0, 4.0, 5.0, 6.0, 7.5, 10.0, 15.0, 25.0, 50.0 μM) were added to **CyR** (5 μM). Figure 2B shows a calibration plot with a correlation coefficient (R^2) of 0.9873 over KO_2 concentration range of 0–7.5 μM. The limit of detection (LOD) was calculated as 9.9 nM (relative standard deviation σ = 0.096, n=3; slope, 29.15). As well, a good linearity was also obtained with R^2 as 0.990 and LOD (relative standard deviation σ = 0.16, n=3) as 15.5 nM by response of **CyR** to X/XO-generated $O_2^{\bullet-}$ concentration range of 0–6.6 μM (Figure S5). In addition, under normal physiological conditions, $O_2^{\bullet-}$ concentrations are usually supposed to be in the lower nanomolar range. However, when an "oxidative stress" exists, an abundance of superoxide will quickly increase up to a higher micromolar range. Hence, these results indicate that **CyR** can be applied to biological samples.

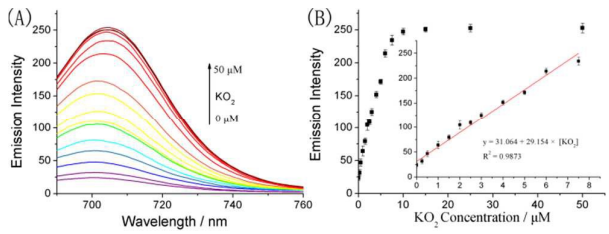

Figure 2. (A) Fluorescence titration of CyR (5 μM) upon addition of KO_2 (0, 0.25, 0.5, 1.0, 1.5, 2.0, 2.5, 3.0, 4.0, 5.0, 6.0, 7.5, 10.0, 15.0, 25.0, 50.0 μM). Each spectrum was recorded at 10 min after addition of KO_2. (B) Inset: A linear correlation between emission intensities and concentrations of KO_2.

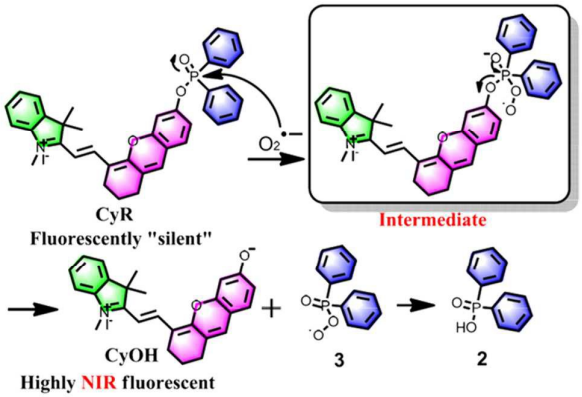

Scheme 2. The proposed recognition mechanism for transformation of **CyR** to **CyOH** by $O_2^{\bullet-}$.

Study on Reaction Mechanism. The mechanism of the reaction of **CyR** with $O_2^{\bullet-}$ was evaluated, and its products were analyzed. According to the well-established reaction mechanism,[10k] signaling occurs due to the selective deprotection of the diphenyl phosphinate group of **CyR** by $O_2^{\bullet-}$ (Scheme 2). Thus, generated **CyOH** showed its featural fluorescent signaling behaviors. In order to further confirm the sensing mechanism, HPLC analysis was carried out (Figure S6), which showed that **CyR** was transformed to **CyOH** by reaction with $O_2^{\bullet-}$. The ESI spectrometry analysis (Figure S7) of **CyR** treated with $O_2^{\bullet-}$ (1.0 equiv) in PBS buffer (10 mM, pH 7.40) containing 5% DMSO also confirms the formation of the expected **CyOH** (m/z 384.2242) and diphenylphosphinic acid **2** (m/z 219.2053). As can been seen from Figure S8, the possible photoinduced electron transfer (PET) process in **CyR** was supported by the LUMO and HOMO levels[16].

Applications. Based on the above results, we tested the potential of **CyR** for its cells imaging applications. As shown in Figure 3, *HepG2* cells incubated with **CyR** (5 μM) for 15 min at 37 °C showed outstanding red fluorescence in the cytoplasm (Figure 3B). This indicated that **CyR** could permeate into cells and reacted with $O_2^{\bullet-}$ to generate distinguishable fluorescence images. In the control test, on the treatment of the cells with a superoxide scavenger Tiron (200 μM) for 20 min, followed by **CyR** (5 μM) for another 15 min, a feeble red fluorescence was observed (Figure 3C). Furthermore, stimulating with 2-ME (2-Methoxyestradiol, an effective experimental $O_2^{\bullet-}$ producing anticancer agent[17]) to the Tiron-pretreated *HepG2* cells and then incubating subsequently with **CyR** (5 μM) for 15 min, led to the enhancement of red fluorescence (Figure 3D). In addition, living *HepG2* cells incubated with **CyR** (5 μM) after treated with Tiron (200 μM), followed by stimulated with 2-ME (100 μM) and then the fluorescence images were recorded at different time points for 10 min. As shown in Figure S9, the fluorescence intensity increased significantly over time. These result confirmed that the red fluorescence in the cytoplasm of *HepG2* cells was due to intracellular $O_2^{\bullet-}$. The cytotoxicity of **CyR** in *HepG2* cells was also performed by MTT assay. The results showed that the cells remained in good condition upon treatment with 0-60.0 μM **CyR** for 24 h (Figure S10). This indicated that **CyR** was of low cytotoxicity to the cultured cells and has great potential for biological applications.

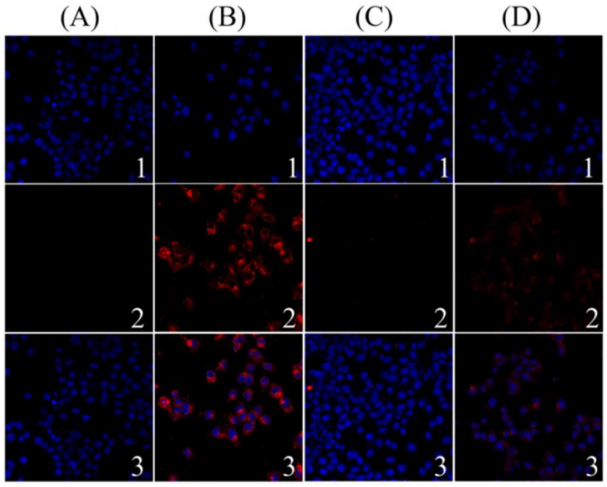

Figure 3. Confocal microscope images of **CyR** in *HepG2* cells co-stained with 4′,6-diamidino-2-phenylindole (DAPI) to identify cell nuclei (blue dots). (A) control; (B) Cells were incubated with **CyR** (5 μM) for 15 min; (C) Image of cells treatment with Tiron (300 μM) for 20 min and subsequent treatment of the cells with **CyR** (5 μM) for 15 min. (D) Image of cells stimulated by 2-ME for 30 min after being incubated with Tiron for 20 min, followed by loading with **CyR** (5 μM) for 15 min. (1) Fluorescence images from DAPI; (2) Fluorescence images from **CyR**; and (3) Merge.

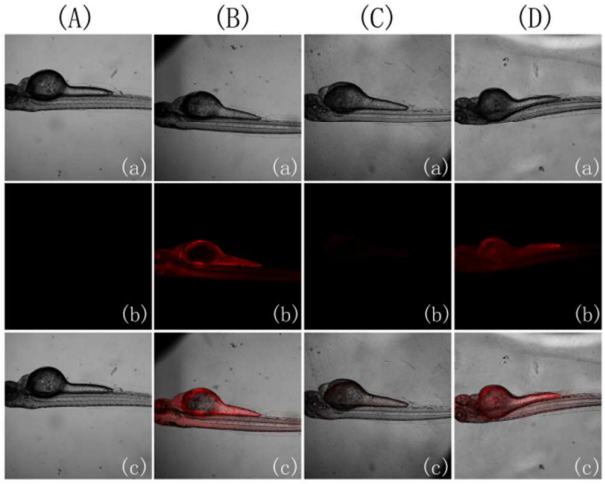

Figure 4. Confocal microscope images of **CyR** in zebrafish (A) control; (B) Image of the zebrafish incubated with **CyR** (5 μM) for 15 min; (C) Image of the zebrafish treatment with Tiron (200 μM) for 20 min and subsequent treatment with **CyR** (5 μM) for 15 min. (D) Image of the zebrafish stimulated by 2-ME for 30 min after incubated with Tiron for 20 min, followed by loading with **CyR** (5 μM) for 15 min. (a)Bright-field; (b) Fluorescence images from **CyR**; and (c) Merge.

Taking advantage of the NIR behavior and high sensitivity of **CyR** toward $O_2^{\bullet-}$, the practical application of **CyR** as a fluorescence probe to monitor $O_2^{\bullet-}$ distribution in live zebrafish was studied. Imaging showed a bright red fluorescence in the abdomen of 3 day old zebrafish (Figure 4B), and a feeble red fluorescence was observed when the zebrafish pretreated with Tiron (Figure 4C). The zebrafish stimulated by 2-ME after incubated with Tiron, followed by incubating with **CyR** exhibited a relatively strong fluorescence (Figure 4D). These results indicate that **CyR** can be used as a fluorescence imaging agent for $O_2^{\bullet-}$ in live zebrafish.

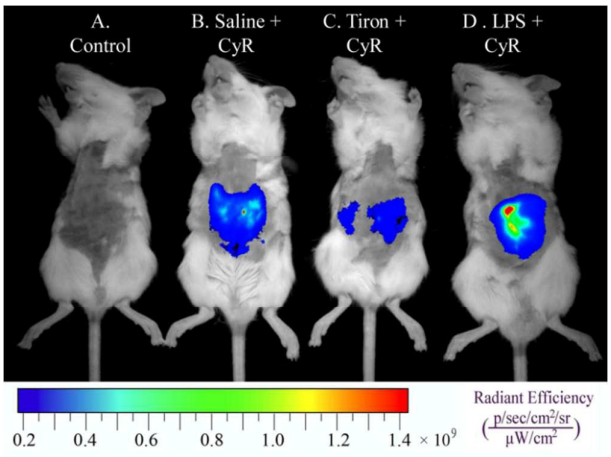

Figure 5. In vivo imaging of ROS production from the peritoneal cavity of mice with **CyR**. Fluorescence images of (A) a mouse that had not been i.p. injected with **CyR** (Control), (B) a mouse injected with **CyR** after being preinjected with Saline (Saline + **CyR**); (C) Tiron was injected in the i.p. cavity of a mouse, followed by i.p. injection of **CyR** (Tiron + **CyR**); (D) LPS was injected into the peritoneal cavity of a mouse, followed by an i.p. injection of **CyR** (LPS + **CyR**); Mouse from each group was imaged at the same time after **CyR** injection.

A key benefit of **CyR** is its long emission wavelength, which makes **CyR** available for bioimaging applications in living animals. Kunming (KM) mice were selected as our model and divided into four groups. As shown in Figure 5, the first group was untreated as a control group; The second group was given an intraperitoneal (i.p.) injection of saline; The third group was given an i.p. injection of Tiron; The last group was given an i.p. injection of lipopolysaccharide endotoxin (LPS).[10e] After 6h, the saline, Tiron, and LPS treated mice were injected i.p. with **CyR**. The mice were imaged as quadruplets after 15 min. The mouse pretreated saline shows remarkable fluorescence images (Figure 5B), while lower fluorescence intensity was monitored when mouse pretreated Tiron (Figure 5C). The mouse pretreated with LPS shows a greater fluorescent intensity (Figure 5D) compared to mouse pretreated with saline, and shows apparent fluorescence enhancement for a certain time (Figure S11). For liver imaging, liver stimulated with LPS presenting higher fluorescence intensity than untreated (Figure S12). With the above results taken together, it was revealed that **CyR** could image ROS production in *in vivo*, and for the first time, in mouse liver.

Conclusions

In summary, we have developed a simple and efficient NIR fluorescence probe for the detection of $O_2^{\bullet-}$ in aqueous solution and imaging in biological environments. The sensitive fluorescent sensor **CyR** has a high selectivity for $O_2^{\bullet-}$ over other intracellular ROSs, biomolecules, and ions. It also can offer high-contrast colorimetric and particular red fluorescence turn-on means for the detection of $O_2^{\bullet-}$ within 10 min with a low detection limit of 9.9 nM and has good function at physiological pH. Furthermore, we have illustrated the value of **CyR** by surveying living-cell-derived $O_2^{\bullet-}$ within normal and 2-ME-stimulated *HepG2* cells. The results showed that **CyR** is a prominent fluorescence probe that possesses good sensitivity, high selectivity, cell membrane permeability, low cytotoxicity, and rapid reactivity toward $O_2^{\bullet-}$. Moreover, we also have successfully applied the probe to detect $O_2^{\bullet-}$ in live zebrafish, mouse and, for the first time, in mouse liver. Herein, the fluorescence probe could be a good candidate for biological applications.

The authors thank Prof. Shaobo, Sun and Prof. Yali, Wang (GanSu University of Chinese Medicine, China) for their technical assistance. This work was supported by National Science Foundation of China (No. 21375052, 21575055).

Notes and references

[1] L. A. Sena and N. S. Chandel, *Molecular cell*, 2012, **48**, 158-167.
[2] W. M. Nauseef, *Semin. Immunopathol.*, 2008, pp. 195-208.
[3] M. Inoue, E. F. Sato, M. Nishikawa, A.-M. Park, Y. Kira, I. Imada and K. Utsumi, *Curr. Med. Chem.*, 2003, **10**, 2495-2505.
[4] a) B. M. Babior, *Curr. Opin. Immunol.*, 2004, **16**, 42-47; b) G. Groeger, C. Quiney and T. G. Cotter, *Antioxid. Redox Sign.*, 2009, **11**, 2655-2671; c) M. Valko, D. Leibfritz, J. Moncol, M. T. Cronin, M. Mazur and J. Telser, *Int. j. Biochem. Cell Biol.*, 2007, **39**, 44-84.
[5] a) C. Nathan and *J. Clin. Invest.*, 2003, **111**, 769; b) B. Halliwell, J. Gutteridge and C. E. Cross, *J. lab. Clin. Med.*, 1992, **119**, 598-620; c) A. P. Wickens, *Respir. Physiol.*, 2001, *128*, 379-391; d) D. C. Wallace, *Science*, 1999, **283**, 1482-1488.
[6] a) B. C. Dickinson and C. J. Chang, *Nat. Chem. Biol.*, 2011, **7**, 504-511; b) A. W. Linnane, M. Kios and L. Vitetta, *Mitochondrion*, 2007, **7**, 1-5; c) C. C. Winterbourn, *Free Radical Bio. Med.*, 1993, **14**, 85-90.
[7] I. A. Abreu and D. E. Cabelli, *BBA-Proteins Proteom.*, 2010, **1804**, 263-274.
[8] a) G. Ferrer-Sueta and R. Radi, *ACS Chem. Biol.*, 2009, **4**, 161-177; b) R. Radi, *J. Biol. Chem.*, 2013, **288**, 26464-26472.
[9] a) M. Yamato, T. Egashira and H. Utsumi, *Free Radical Biol. Med.*, 2003, **35**, 1619-1631; b) W. M. Armstead, *Brain Res.*, 2001, **910**, 19-28; c) Y. Saito, Y. Yoshida, T. Akazawa, K. Takahashi and E. Niki, *J. Biol. Chem.*, 2003, **278**, 39428-39434; d) G. M. Rosen and B. A. Freeman, *P. Natl. Acad. Sci.*, 1984, **81**, 7269-7273; e) H. Yasui and H. Sakurai, *Biochem. Bioph. Res. Co.*, 2000, **269**, 131-136.
[10] a) S. Ma, W. Mu, J. Gao and J. Zhou, *J. Fluoresc.*, 2009, **19**, 487-493; b) W. Zhang, P. Li, F. Yang, X. Hu, C. Sun, W. Zhang, D. Chen and B. Tang, *J. Am. Chem. Soc.*, 2013, **135**, 14956-14959; c) S. T. Manjare, S. Kim, W. D. Heo and D. G. Churchill, *Org. Lett.*, 2014, **16**, 410-412; d) J. J. Gao, K. H. Xu, B. Tang, L. L. Yin, G. W. Yang and L. G. An, *FEBS J.*, 2007, **274**, 1725-1733; e) F. Yu, M. Gao, M. Li and L. Chen, *Biomaterials*, 2015, **63**, 93-101; f) W. Zhang, X. Wang, P. Li, F. Huang, H. Wang, W. Zhang and B. Tang, *Chem. Commun.*, 2015, **51**, 9710-9713; g) F. Si, Y. Liu, K. Yan and W. Zhong, *Chem. Commun.*, 2015, **51**, 7931-7934; h) D. P. Murale, H. Kim, W. S. Choi and D. G. Churchill, *Org. Lett.*, 2013, **15**, 3946-3949; i) H. Maeda, K. Yamamoto, Y. Nomura, I. Kohno, L. Hafsi, N. Ueda, S. Yoshida, M. Fukuda, Y. Fukuyasu and Y. Yamauchi, *J. Am. Chem. Soc.*, 2005, **127**, 68-69; j) K. Xu, X. Liu, B. Tang, G. Yang, Y. Yang and L. An, *Chem.-Eur. J.*, 2007, **13**, 1411-1416; k) K. Xu, X. Liu and B. Tang, *ChemBioChem*, 2007, **8**, 453-458; l) Y. Yang, Q. Zhao, W. Feng and F. Li, *Chem. Rev.*, 2012, **113**, 192-270.
[11] D. J. Stephens and V. J. Allan, *Science*, 2003, **300**, 82-86.
[12] P. Gallop, M. Paz, E. Henson and S. Latt, *BioTechniques*, 1984, **1**, 32-36.
[13] C. Bucana, I. Saiki and R. Nayar, *J. Histochem. Cytochem.*, 1986, **34**, 1109-1115.
[14] G. Rothe and G. Valet, *J. Leukocyte Biol.*, 1990, **47**, 440-448.
[15] Y. Fang and R. Zheng, *Theory and Application of Free Radical Biology,* Scientific Press, Beijing 2002, p. 191.
[16] a) J. Zhang, J. Wang, J. Liu, L. Ning, X. Zhu, B. Yu, X. Liu, X. Yao and H. Zhang, *Anal. Chem.*, 2015, **87**, 4856-4863; b) J. Zhang, B. Yu, L. Ning, X. Zhu, J. Wang, Z. Chen, X. Liu, X. Yao, X. Zhang and H. Zhang, *Eur. J. Org. Chem.*, 2015, **2015**, 1711-1718.
[17] Y. Zhou, E. O. Hileman, W. Plunkett, M. J. Keating and P. Huang, *Blood*, 2003, **101**, 4098-4104.